Chapter 6

Thermal Measurements from the Gulf of Mexico Continental Slope: Results from the PAGE Cruise

Cinthia Labails[1], Louis Géli[1], Nabil Sultan[1], Ivana Novosel[2], and William J. Winters[3]

Thermal measurements from the Gulf of Mexico continental slope: Results from the PAGE cruise; chapter 6 in *Winters, W.J., Lorenson, T.D., and Paull, C.K., eds., 2007, Initial report of the IMAGES VIII/PAGE 127 gas hydrate and paleoclimate cruise on the RV* Marion Dufresne *in the Gulf of Mexico, 2–18 July 2002: U.S. Geological Survey Open-File Report 2004–1358.*

Abstract

In July 2002, the French Polar Institute (Institut Polaire Francais – Paul-Emile Victor (IPEV)) and the U.S. Geological Survey jointly conducted a cruise aboard the research vessel (RV) *Marion Dufresne* to collect giant piston cores to determine the distribution of gas hydrate in the northern Gulf of Mexico. Thermal measurements (made by Ifremer, using autonomous digital temperature probes fitted on gravity-core barrels) were successfully used to calculate a geothermal gradient at 17 sites. Geothermal gradients varied from 20 to 38 degrees Celsius per kilometer.

Introduction

To determine the thermodynamic conditions (temperature and pressure) at which gas hydrate is stable in reservoir sediments at depth and to assess the potential amount of gas hydrate in the Gulf of Mexico, heat-flow measurements were made in three areas: Tunica Mound (fig. 1), Bush Hill (fig. 2), and proximally to the Mississippi Canyon (fig. 3). Because the main objective of the cruise was the acquisition of giant piston cores, only a limited number of thermal measurements were made at each site by using autonomous digital temperature probes (fig. 4) fitted onto gravity-core barrels. A total of 21 deployments were made (table 1), resulting in the calculation of 17 geothermal gradients. Four deployments were unsuccessful because of bent barrels or inadequate penetration.

Equipment, Data Reduction, and Processing

Equipment. Temperature measurements were made using autonomous temperature probes welded onto gravity-core barrels. The probes incorporate an energy source and are able to record a total of 26,280 acquisitions. Most measurements were made in water depths ranging between about 600 and 1,200 meters (m). Because temperatures in the few upper meters of sediments could be affected by seasonal changes in bottom water temperatures, the thermal sensors were placed so as to record temperatures deeper than this transitional shallow subbottom zone. The sensors were fitted onto 17- to 21-m-long gravity core barrels (except at one site, where a 12-m-long barrel was used). The inclination of the barrel was measured using a tiltmeter installed on the corer weight stand. Mud recovered on the corer weight stand typically indicated that full penetration of the gravity corer was achieved at most sites (except for sites where barrels were bent). Thermal gradients were computed using probe depths calculated from the tilt measurements and the probe relative spacing.

Probe Intercalibration. Before each core-barrel penetration, temperature probes were intercalibrated for 3 minutes in the water column by measuring temperature for each sensor as the core barrel was suspended 150 m and 100 m above the sea floor. With these two intercalibrations, it is possible to calculate the temperature difference measured by two different sensors placed at the same water depth. After each core penetration, temperatures were again measured for 3 minutes

[1]Department of Marine Geosciences, Ifremer, BP 70, 29280, Plouzané, France.

[2]Rice University, Department of Earth Sciences, 6100 Main Street, MS-126, Houston, TX 77005-1892 USA.

[3]U.S. Geological Survey, 384 Woods Hole Road, Woods Hole, MA 02543 USA.

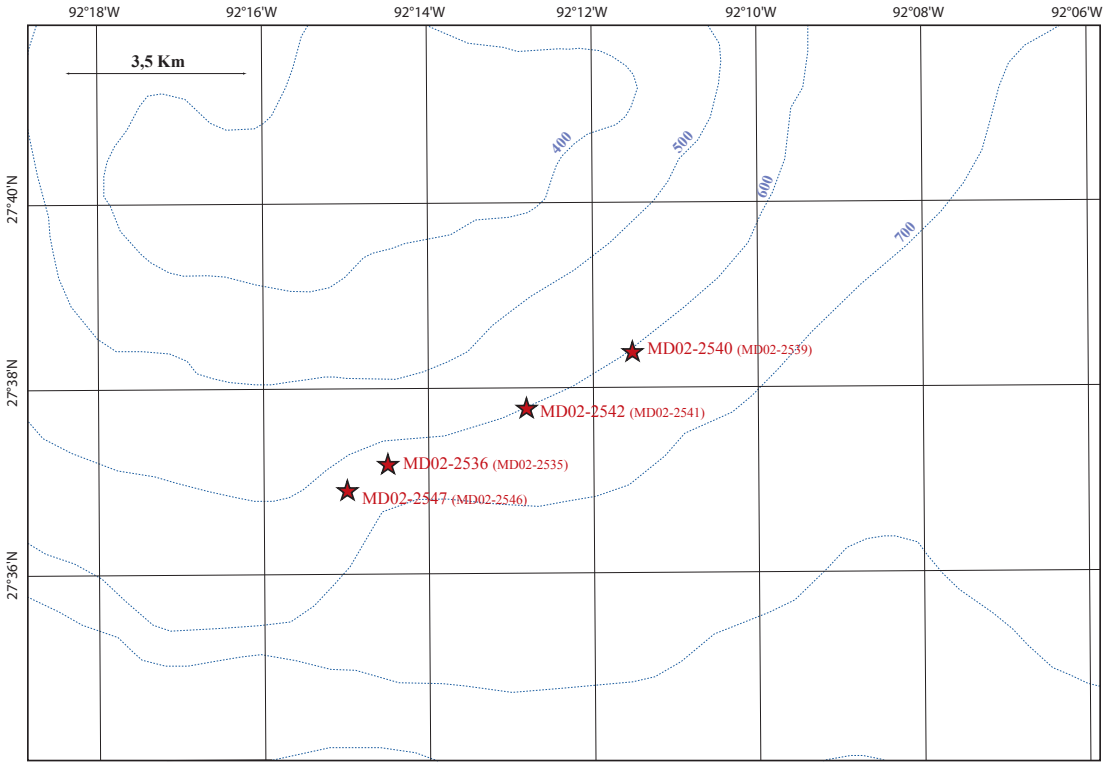

Figure 1. Tunica Mound sites for thermal measurements. The closest Calypso cores that were used for conductivity measurements and heat-flow calculations are in parentheses.

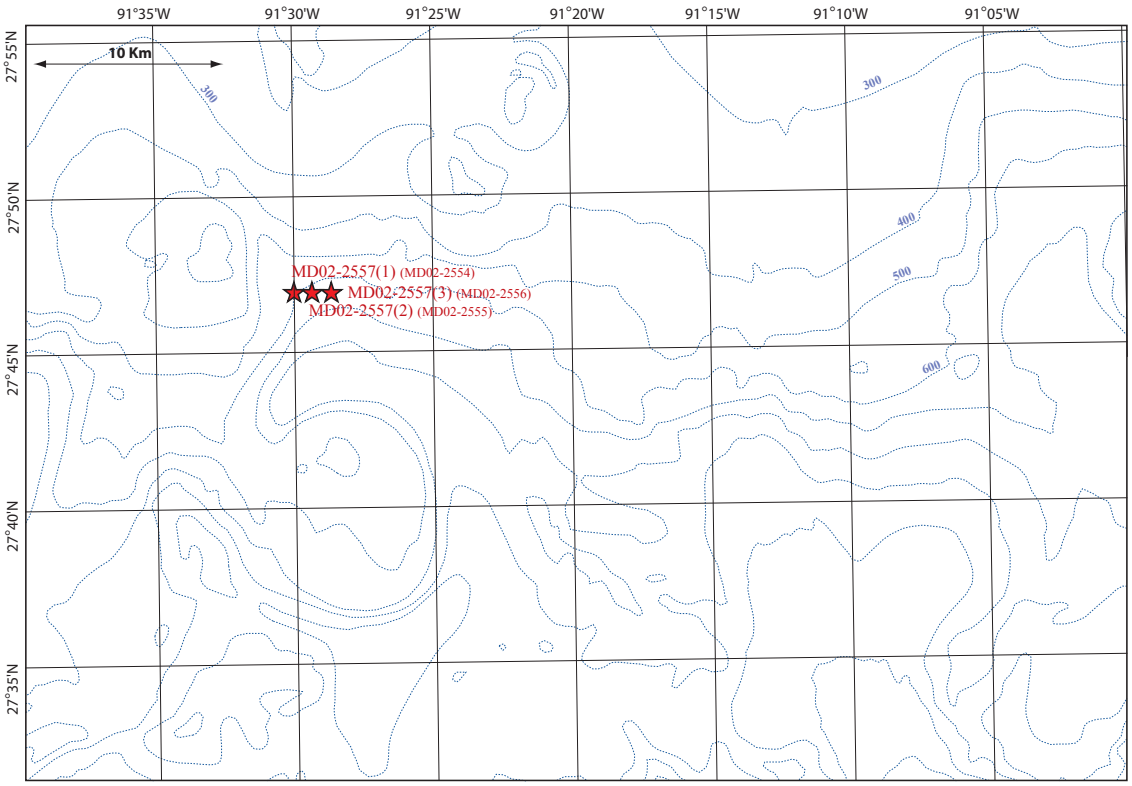

Figure 2. Bush Hill sites for thermal measurements. The closest Calypso cores that were used for conductivity measurements and heat-flow calculations are in parentheses.

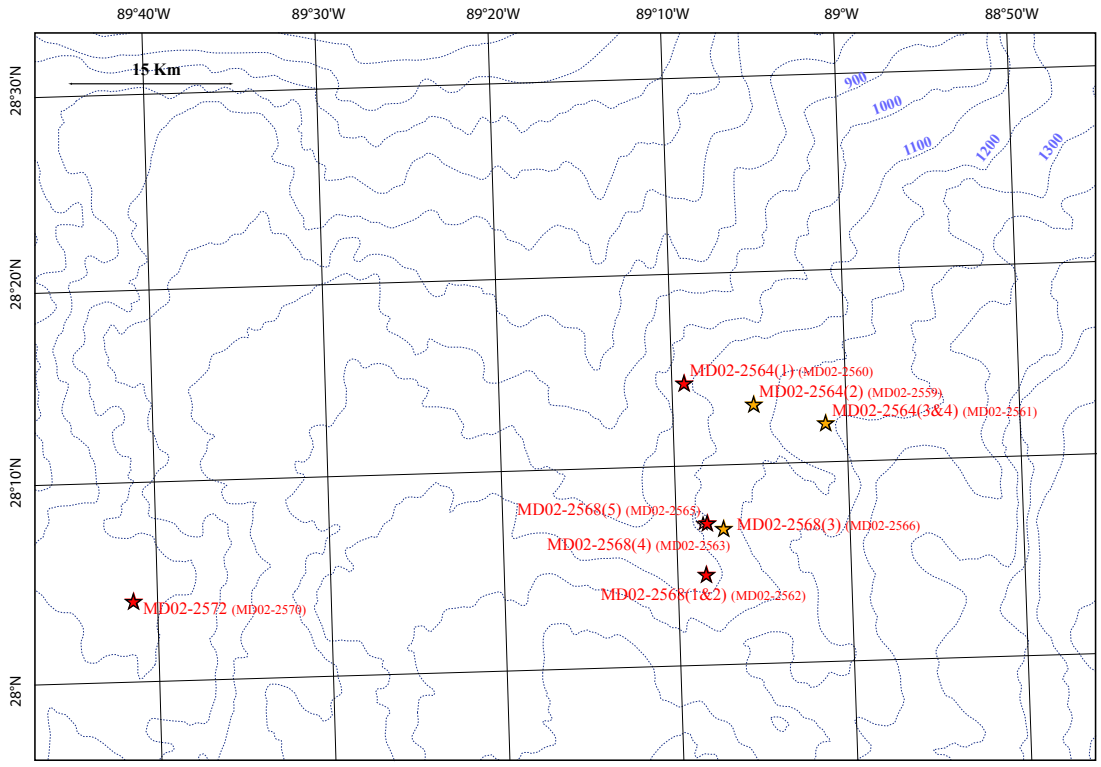

Figure 3. Mississippi Canyon region sites for thermal measurements. The closest Calypso cores that were used for conductivity measurements and heat-flow calculations are in parentheses.

Figure 4A. Gravity corer of RV *Marion Dufresne* equipped with autonomous temperature probes. Thermal sensors are rotated along the core barrel to avoid disturbing effects from one sensor to the other during penetration.

Figure 4B. A Micrel autonomous temperature sensor welded onto a gravity-core barrel. Because the sensor is fully self contained, there is no connector and no power switch. Dialog is performed using a reading pen connected to the serial port of a personal computer. Batteries and a data logger are contained in a 172-millimeter (mm)- long, 28-mm-diameter titanium cylinder. Two temperature probes are contained in a 130-mm-long, 4-mm-diameter titanium needle. The probe is located 60 mm from the core barrel. This distance ensures that it will take 1 hour for the heat generated by the friction of penetration to reach the needle probe. Probe temperature range: –2 to 35 degrees Celsius (°C); linearity: ±2 milli-degrees Celsius (m°C); resolution: 0.6 m°C; stability: 20 m°C/year; repeatability: ±0.6 m°C; total measurement range: –2 to 75 °C ; maximum water depth: 6,000 meters (m).

Table 1. Summary of thermal measurements.

[m, meters; N, north; W, west; °C/km, degrees Celsius per kilometer; k_a, average thermal conductivity; $Wm^{-1}K^{-1}$, watt per meter Kelvin; mW/m^2, milliwatt per meter squared; mfbc, meters from bottom of corer; TM, Tunica Mound; POGO, multiple pogo-like penetrations; BH, Bush Hill; MC, Mississippi Canyon. "Average" conductivity and "average" heat flow are defined in the text. Because gravity core recovery ratios typically did not exceed 50 to 70 percent, the nearest giant (Calypso) piston core was used to estimate thermal conductivity over a depth of 35 meters, while temperature measurements were collected only over the length of the gravity corer (~17 to 20 meters long)]

Area	Nearest giant piston (Calypso) core MD02-	Length of Calypso piston core (m)	Name of heat-flow measurement MD02-	Latitude (N)	Longitude (W)	Water depth (m)	Thermal gradient (°C/km)	Average thermal conductivity k_a ($Wm^{-1}K^{-1}$)	Heat flow (Bullard) (mW/m^2)	Average heat flow (mW/m^2)	Core length (m)	Observations (mfbc)
TM	2535	37.6	2536(1)	27°37.19'	92°14.46'	608	23 ± 2	0.99 ± 0.07	23 ± 2	22 ±4	8.88	
TM			2536(2)	27°37.52'	92°14.76'	564	26 ± 2			26 ± 4		POGO (natural drift).
TM			2536(3)	27°37.62'	92°14.25'	585	26 ± 2			26 ± 4		POGO (natural drift).
TM	2539	30.7	2540(1)	27°38.42'	92°11.52'	617	38 ± 5	1.01 ± 0.08	39 ± 5	36 ± 8	5.65	Uncertainty in inclination.
TM			2540(2)	27°38.41'	92°11.71'	620						Corer bent 15 mfbc; no measurements.
TM	2541	35.7	2542	27°37.93'	92°12.72'	617	25 ± 1	1.01 ± 0.09	27 ± 2	26 ± 3	7.70	
TM	2546	30.6	2547	27°36.99'	92°14.90'	607	29 ± 1	0.92 ± 0.07	25 ± 1	27 ± 3	5.69	Corer bent 12 mfbc; data OK.
BH	2554	30.3	2557(1)	27°46.98'	91°29.92'	613	29 ± 1	0.91 ± 0.16	28 ± 3	27 ± 6	7.59	
BH	2555	24.9	2557(2)	27°46.98'	91°29.34'	639	25 ± 1	0.98 ± 0.09	23 ± 1	25 ± 3		
BH	2556	23.3	2557(3)	27°46.97'	91°28.83'	659	25 ± 1	0.97 ± 0.08	24 ± 1	24 ± 3		
MC	2560	22.6	2564(1)	28°14.60'	89°9.27'	1,027	32 ± 1	0.94 ± 0.13	30 ± 1	30 ± 5	7.63	
MC	2559	23.7	2564(2)	28°13.34'	89°05.30'	1,261	35 ± 1	1.02 ± 0.14	32 ± 1	35 ± 6		
MC	2561	28.7	2564(3)	28°12.31'	89°01.20'	1,269	38 ± 1	0.96 ± 0.18	36 ± 1	37 ± 8		
MC			2564(4)	28°12.42'	89°01.20'	1,269	38 ± 1	0.96 ± 0.18		37 ± 8		POGO (natural drift).
MC	2562	25.8	2568(1)	28°04.74'	89°08.40'	1,049	22 ± 1	1.03 ± 0.09	23 ± 1	23 ± 3	6.96	
MC			2568(2)	28°04.86'	89°08.22'	1,057	20 ± 2	1.03 ± 0.09		21 ± 3		POGO (natural drift).
MC	2566	25.8	2568(3)	28°07.16'	89°06.18'	1,190	33 ± 1	0.99 ± 0.08	32 ± 1	32 ± 4		
MC	2565		2568(4)	28°07.40'	89°08.37'	1,068						Bad penetration; no measurements.
MC	2563		2568(5)	28°07.41'	89°08.17'	1,049						Corer bent 9 mfbc; bad penetration; no measurements.
MC	2570	20.9	2572	28°04'.26'	89°41.39'	628	36 ± 3	0.79 ± 0.11	26 ± 3	28 ± 5	4.9	Full penetration; mud on core weight.
MC	2569		2573	28°9.11'	89°28.79'	1,027					4.2	Corer bent 9 mfbc; bad penetration; no measurements.

in the water column, 100 m above sea floor. This second check ensured that all sensors were functioning properly after penetration.

Thermal Gradients. To reduce the effect of frictional heating produced by the penetration of probes into the sea floor (Bullard, 1954; Jaeger, 1965), the core remained embedded in the sea floor for more than 6 minutes to allow collection of baseline data. The exact duration of the measurements was a function of the behavior of the corer cable. The cable tension was measured in real time to ensure that no tension was applied during the measurement period. Temperature and time plots were produced to estimate the background sediment temperature [for example, (Lister, 1970; Hyndman and others, 1979; Villinger and Davis, 1987)].

Thermal Conductivity. Even when full penetration of the gravity corer was achieved (providing sediment temperatures over the full corer length), simultaneously recovered sediment cores generally were shorter than 6 to 9 m long. For this reason, thermal measurements (except multiple POGO-like penetrations were made as close as possible to Calypso piston core sites, and thermal conductivities were measured on the piston cores by using a needle probe technique (such as Von Herzen and Maxwell, 1959). Measurements were made every 1.5 m (one measurement per core section) after thermal equilibrium of the core was reached. In one single piston core, the variability typically was greater than about 20 to 25 percent. We, therefore, computed different mean values of thermal conductivity (Novosel and others, this volume, chapter 7) :

– equivalent mean conductivity (k_e):

$$k_e = \frac{\Delta Z}{\sum \frac{\Delta Z_i}{k_i}} \tag{1}$$

– harmonic mean conductivity (k_h):

$$k_h = \frac{n}{\sum \frac{1}{k_i}} \tag{2}$$

– arithmetic mean conductivity (k_a):

$$k_a = \frac{1}{n} \sum k_i \tag{3}$$

where Δz_i and ki are the spacing and the thermal conductivity, respectively, between probes I and I+1.

Heat-Flow Measurements. Two heat-flow values (q_e and q_a) were computed (table 1) :

– the Bullard heat flow (q_e) was obtained by plotting temperature (T) with integrated thermal resistance at depth (z) (Bullard, 1954) :

$$q_e = \frac{dT}{d\xi} \tag{4}$$

where

$$\xi = \sum_{i=0}^{N} R_i \Delta Z_i \quad with \quad R_i = \frac{1}{k_i} \tag{5}$$

and k_i is the measured conductivity at a given core section number (i).

– the average heat flow (q_a) was determined from:

$$q_a = G \times k_a \tag{6}$$

where G is the average thermal gradient estimated by linear regression on the (T, z) plot; and k_a is the arithmetic mean conductivity.

– the error for q_a can be determined from:

$$\frac{\Delta q_a}{q_a} = \frac{\Delta k_a}{k_a} + \frac{\Delta G}{G} \tag{7}$$

Summary of Results and General Remarks

At a number of sites, several heat-flow measurements (POGO-like) were made by reentering the corer into the sea floor several times during the same lowering (reentries were made after the ship drifted for about 15 to 20 minutes). This procedure provided additional information on local variability but used little ship time. Previous experience indicates that the corer can easily penetrate several times into the sea floor and that this typically does not adversely affect the core sampled during the first penetration. Results are summarized in table 1 and figures 5 and 6. Thermal measurements are presented in table 2. Thermal conductivities are reported separately by Novosel and others (this volume, chapter 7).

(1) In the Tunica Mound and Bush Hill areas (figs. 1 and 2), water depths ranged between 564 and 659 m. Except for the bottom two temperature readings at site MD02-2540 GHF, the temperature and depth profiles all were relatively linear. The measured thermal gradients (obtained by fitting a regression line to the temperature and depth plots for depths >2 m) ranged between 23 and 29 degrees Celsius per kilometer (°C/km), except at site MD02-2540 GHF, where a value of 38 °C/km was determined.

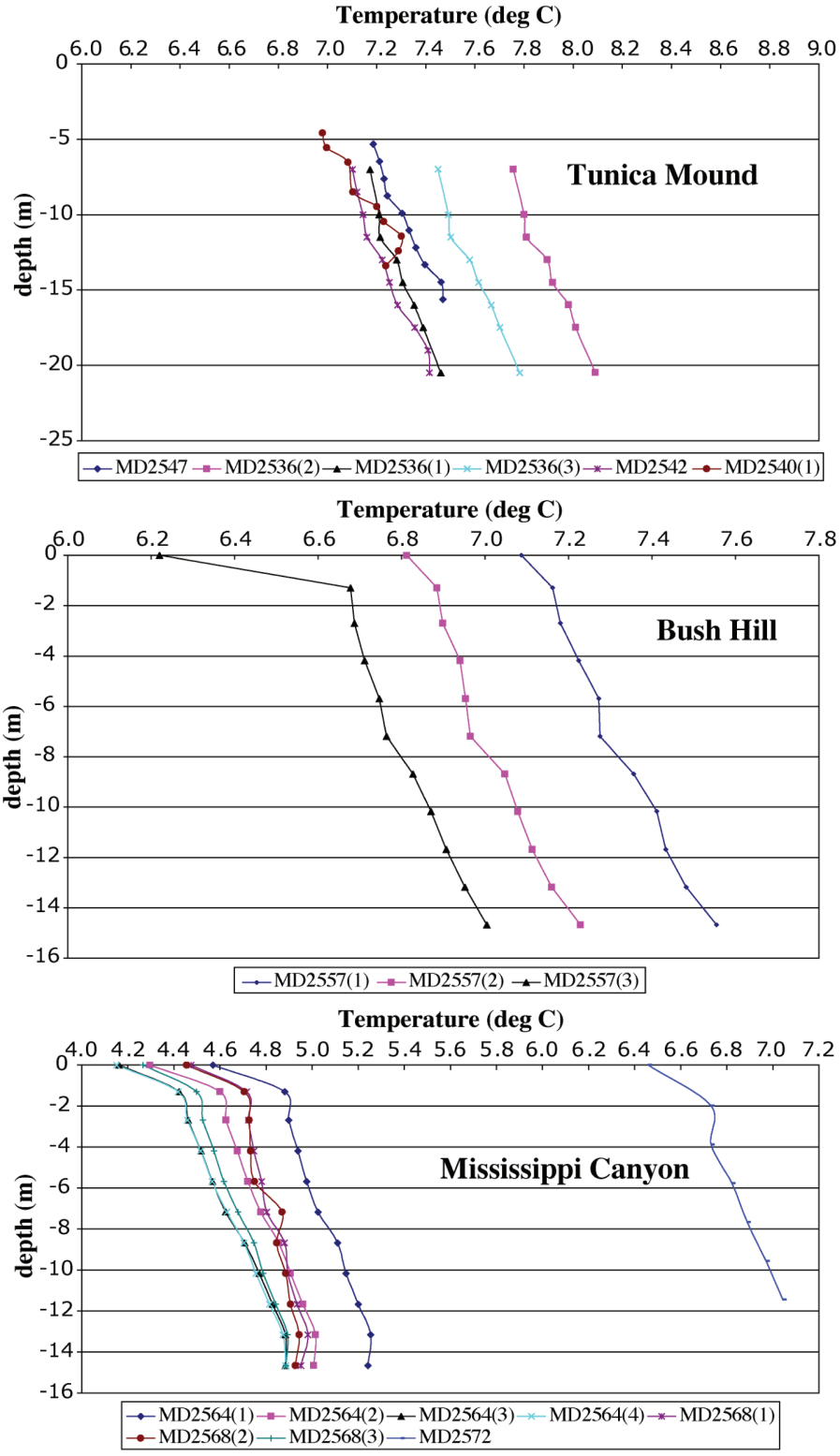

Figure 5. Temperature versus depth profiles for each study area.

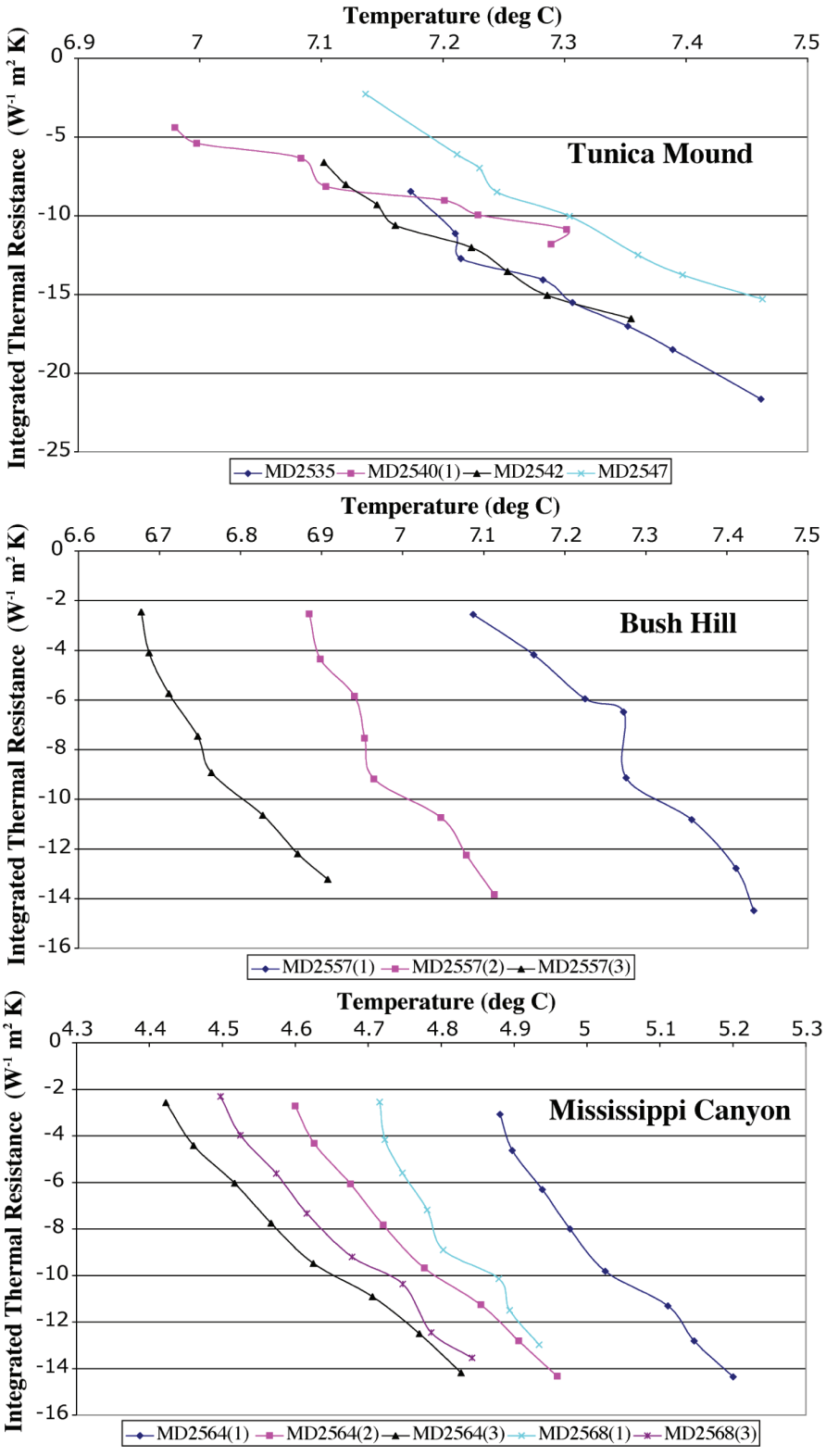

Figure 6. Temperature versus integrated thermal resistance curves for each study area. At a number of sites, several heat-flow measurements were made (POGO-like) by reentering the corer into the sea floor several times during the same lowering. Thus, there are fewer plots here than in figure 5, and there is no one-to-one correspondence between symbols in both figures. At the site of the first penetration of the gravity core, one Calypso piston core was collected, generally with 100% recovery. Because the core recovery ratio of the gravity cores hardly exceeded 70%, shipboard thermal conductivity measurements were performed on the Calypso giant piston core rather than on the gravity core.

Table 2. Temperature measurements.

[N, north; W, west; T_0, bottom water temperature; m, meters; C, degrees Celsius; GB-GC, Garden Banks-Green Canyon (Tunica Mound); NaN, not a valid number; BH, Bush Hill; MC, Mississippi Canyon]

Area	Name of Calypso core MD02-	Name of heat-flow measurement MD02-	Latitude (N)	Longitude (W)	Depth (m)	T_0	Depth											Temperature										
							d1 (m)	d2 (m)	d3 (m)	d4 (m)	d5 (m)	d6 (m)	d7 (m)	d8 (m)	d9 (m)	d10 (m)	d11 (m)	T1 (°C)	T2 (°C)	T3 (°C)	T4 (°C)	T5 (°C)	T6 (°C)	T7 (°C)	T8 (°C)	T9 (°C)	T10 (°C)	T11 (°C)
GB -GC	2535	2536(1)	27°37.19'	092°14.46'	608	8.266	7	10	11.5	13	14.5	16	17.5	20.5				7.173	7.210	7.215	7.282	7.306	7.352	7.389	7.462			
GB -GC		2536(2)	27°37.52'	092°14.76'	564	8.692	7	10	11.5	13	14.5	16	17.5	20.5				7.757	7.780	7.809	7.895	7.916	7.981	8.001	8.089			
GB -GC		2536(3)	27°37.62'	092°14.25'	585	8.692	7	10	11.5	13	14.5	16	17.5	20.5				7.451	7.491	7.502	7.579	7.616	7.667	7.702	7.783			
GB -GC	2539	2540(1)	27°38.42'	092°11.52'	617	6.570	4.58	5.56	8.5	10.46	11.44	12.42	13.4					6.979	6.997	7.104	7.229	7.302	7.289	7.238				
GB -GC		2540(2)	27°38.41'	092°11.71'	620	NaN	NaN	NaN	NaN	NaN	NaN	NaN	NaN					NaN	NaN	NaN	NaN	NaN	NaN	NaN				
GB -GC	2541	2542	27°37.93'	092°12.72'	617	6.401	7	8.5	10	11.5	13	14.5	16	17.5	19.0	20.5		7.102	7.120	7.146	7.161	7.223	7.253	7.286	7.355	7.409	7.416	
GB -GC	2546	2547	27°36.99'	092°14.90'	607	7.111	5.33	6.48	7.62	8.76	9.90	11.05	12.19	13.33	14.47	15.62		7.186	7.212	7.230	7.244	7.304	7.332	7.360	7.397	7.463	7.470	
BH	2554	2557(1)	27°46.98'	091°29.92'	613	7.087	1.3	2.7	4.2	5.7	7.2	8.7	10.2	11.7	13.2	14.7	16.2	7.162	7.181	7.225	7.272	7.276	7.356	7.411	7.433	7.482	7.555	7.578
BH	2555	2557(2)	27°46.98'	091°29.34'	639	6.812	1.3	2.7	4.2	5.7	7.2	8.7	10.2	11.7	13.2	14.7	16.2	6.885	6.898	6.941	6.953	6.964	7.047	7.079	7.113	7.160	7.229	7.232
BH	2556	2557(3)	27°46.97'	091°28.83'	659	6.220	1.3	2.7	4.2	5.7	7.2	8.7	10.2	11.7	13.2	14.7	16.2	6.677	6.687	6.711	6.747	6.764	6.827	6.870	6.907	6.952	7.005	7.014
MC	2560	2564(1)	28°14.60'	089°09.27'	1,027	4.570	1.3	2.7	4.2	5.7	7.2	8.7	10.2	11.7	13.2	14.7	16.2	4.881	4.897	4.939	4.977	5.025	5.111	5.147	5.200	5.254	5.242	5.350
MC	2559	2564(2)	28°13.34'	089°05.30'	1,261	4.296	1.3	2.7	4.2	5.7	7.2	8.7	10.2	11.7	13.2	14.7	16.2	4.599	4.626	4.676	4.721	4.777	4.855	4.907	4.959	5.014	5.006	5.111
MC	2561	2564(3)	28°12.31'	089°01.20'	1,269	4.162	1.3	2.7	4.2	5.7	7.2	8.7	10.2	11.7	13.2	14.7	16.2	4.423	4.461	4.517	4.567	4.625	4.706	4.770	4.827	4.883	4.884	4.987
MC		2564(4)	28°12.42'	089°01.20'	1,269	4.151	1.3	2.7	4.2	5.7	7.2	8.7	10.2	11.7	13.2	14.7	16.2	4.419	4.459	4.516	4.565	4.629	4.704	4.756	4.814	4.873	4.885	4.995
MC	2562	2568(1)	28°04.74'	89°08.40'	1,049	4.474	1.3	2.7	4.2	5.7	7.2	8.7	10.2	11.7	13.2	14.7	16.2	4.716	4.723	4.747	4.781	4.803	4.879	4.984	4.934	4.981	4.952	5.039
MC		2568(2)	28°04.86'	89°08.22'	1,057	4.455	1.3	2.7	4.2	5.7	7.2	8.7	10.2	11.7	13.2	14.7	16.2	4.705	4.726	4.733	4.750	4.870	4.846	4.884	4.907	4.943	4.927	5.016
MC	2566	2568(3)	28°07.16'	89°06.18'	1,190	4.265	1.3	2.7	4.2	5.7	7.2	8.7	10.2	11.7	13.2	14.7	16.2	4.498	4.525	4.574	4.616	4.678	4.747	4.787	4.843	4.893	4.885	4.989
MC	2565	2568(4)	28°07.40'	89°08.37'	1,068		NaN	NaN	NaN	NaN	NaN	NaN	NaN	NaN	NaN	NaN	NaN	NaN	NaN	NaN	NaN	NaN	NaN	NaN	NaN	NaN	NaN	NaN
MC	2563	2568(5)	28°07.41'	89°08.17'	1,049		NaN	NaN	NaN	NaN	NaN	NaN	NaN	NaN	NaN	NaN	NaN	NaN	NaN	NaN	NaN	NaN	NaN	NaN	NaN	NaN	NaN	NaN
MC	2570	2572	28°04'.26'	89°41.39'	628	6.459	2.0	3.9	5.8	7.7	9.6	11.5						6.730	6.732	6.822	6.888	6.971	7.044					
MC	2569	2573	28°09.11'	89°28.79'	1,027		NaN	NaN	NaN	NaN	NaN	NaN						NaN	NaN	NaN	NaN	NaN	NaN					

Note: Values of bottom water temperature (T_0) measured at sites M02-2536 (1 to 3) are uncertain, possibly due to the heat capacity of the corer weight stand.

(2) In the Mississippi Canyon area (fig. 3), one successful measurement (MD02-2572 GHF) was obtained on the western side of the canyon. Seven measurements were obtained on the eastern side of the canyon: two (MD02-2568 GHF-1 and GHF-2) were made on a small apron, at water depths of about 1,050 m; the other five measurements were made in a valley adjacent to the main canyon. At all sites, recent changes in bottom water temperature affected the temperature of the uppermost sediment layer (at depths <1.5 m). Temperature and depth profiles all were relatively linear, except for MD02-2568 GHF-1 and GHF-2. At these sites, the temperature and depth profiles were less linear in the T-z (fig. 5) and T-R spaces (fig. 6) than at all other sites.

Measured thermal gradients (obtained by fitting a regression line to the temperature and depth plots for depths >1.5 m) ranged between 32 and 38 °C/km, except for MD02-2568 GHF-1 and GHF-2, where low values of 22 and 20 °C/km, respectively, were determined. Except for these two values, gradients were relatively uniform, with an average of about 35 ± 3 °C/km.

Conclusions

The data reported here provide robust, first-order estimations of the geothermal gradient in the northern Gulf of Mexico. These results are critical for determining the thermodynamic conditions related to gas hydrate stability. Further studies are needed to understand the observed variability and the processes that affect the measured temperature-depth profiles, such as variations in bottom water temperature, small-scale heterogeneities within the sediments, and vertical advection of pore water.

Acknowledgments

At-sea help was provided by the IMAGES (International Marine Past Global Changes Study) and PAGE (Paleoceanography of the Atlantic and Geochemistry) programs, and by IPEV personnel onboard the RV *Marion Dufresne*. Funding was provided by the U.S. Department of Energy Gas Hydrate Program.

References

Bullard, E.C., 1954, The flow of heat through the floor of the Atlantic Ocean: Proceedings of the Royal Society of London, v. 222, p. 408–429.

Hyndman, R.D., Davis, E.E., and Wright, J.A., 1979, The measurement of marine geothermal heat flow by a multipenetration probe with digital acoustic telemetry and in-situ thermal conductivity: Marine Geophysical Research, v. 4, p. 181–205.

Jaeger, J.C., 1965, Application of the theory of heat conduction to geothermal measurements, *in* Smith, W.E., ed., Terrestrial heat flow: American Geophysical Union, Geophysical Monograph, v. 8, p. 7–21.

Lister, C.R.B., 1970, Heat flow west of the Juan de Fuca Ridge: Journal of Geophysical Research, v. 75, p. 2648–2654.

Villinger, H., and Davis, E.E., 1987, A new reduction algorithm for marine heat flow measurements: Journal of Geophysical Research, v. 92, p. 12846–12856.

Von Herzen, R.P., and Maxwell, A.E., 1959, The measurement of thermal conductivity of deep- sea sediments by a needle-probe method: Journal of Geophysical Research, v. 64, p. 1557–1563.